American Mineralogist, Volume 61, pages 248–259, 1976

The electrical resistivity of galena, pyrite, and chalcopyrite

DONALD F. PRIDMORE AND RALPH T. SHUEY

Department of Geology and Geophysics, University of Utah
Salt Lake City, Utah 84112

Abstract

The sulfides galena, chalcopyrite, and pyrite are semiconductors whose electrical resistivity and type are controlled by deviations from stoichiometry and impurity content, and hence by their geochemical environment. We measured electrical resistivity, type, and the impurity content (emission spectrograph and microprobe) on small volumes of sample. Our results, together with those obtained from a comprehensive literature analysis, are used to construct histograms of the natural variability in carrier density and resistivity.

Sulfur deficiency is the dominant defect in chalcopyrite and hence almost all natural samples are *n*-type. It appears that the copper/iron ratio is also important electrically, the copper-rich samples being the more resistive.

Important donor defects in galena (*n*-type samples) are antimony and bismuth impurities, and sulfur vacancies; acceptor defects (*p*-type samples) include silver impurities and lead vacancies. *P*-type samples appear to be restricted to 'Mississippi Valley' and argentiferous deposits.

In pyrite, electrically active impurities include cobalt, nickel, and copper as donors, and arsenic as an acceptor. Deviations from stoichiometry, in the same sense as galena, may be important. Pyrites from sedimentary and epithermal deposits are usually *p*-type if cupriferous sulfides are not present. Samples from hypothermal deposits are usually *n*-type if there are no arsenic minerals in the assemblage.

Introduction

The sulfides galena, chalcopyrite, and pyrite are semiconductors. The semiconductivity is due to free charge carriers, for which three sources may be distinguished: (1) deviation from stoichiometry, (2) trace elements in solid solution, and (3) thermal excitation across the energy gap. The energy gaps of galena, chalcopyrite, and pyrite are 0.4, 0.6, and 0.9 electron volts, respectively (for references see Shuey, 1975, Chapters 11, 13, 16); therefore, the contribution of the last source is negligible at room temperature. The crystal defects which produce the carriers in these sulfides can be classified as either donors or acceptors, depending on whether they "donate" electrons to the conduction band or "accept" electrons from the valence band, leaving a hole. Unless the concentrations of donors and acceptors are almost exactly equal, the carriers are of predominantly one type. The semiconduction is termed *n*-type or *p*-type according to whether electrons or holes are dominant.

The main objective of the research reported in this paper was to determine the sources of free carriers in pyrite, chalcopyrite, and galena; in particular to identify the dominant donors and acceptors, and understand the geologic factors which may control their concentrations. Our experimental method consisted of measuring the resistivity and thermoelectric voltage on a suite of specimens of diverse geological origin. The resistivity is proportional to the product of the carrier concentration and mobility, while the thermoelectric voltage gives carrier type and some information about the carrier concentration. On the basis of these measurements, representative samples were selected for chemical analysis (spectrograph and microprobe) to identify the electrically active impurities.

In recent years there have been numerous published measurements of resistivity, thermoelectricity and impurity, particularly in pyrite (*e.g.*, Fischer and Hiller, 1956, Favorov *et al.*, 1972). Rarely have all three kinds of data been collected on the same specimen. As we report our experimental results, we indicate when a similar result has been previously published. For our interpretations we draw upon all available data, our own and that already published.

Electrical measurement procedure

The thermoelectric and resistivity measurements were made with a linear, four-needle probe (Signatone Co.). The steel needles were spaced 0.63 mm apart, with tip radius 2.54 μm, and loaded to 80 gm per needle. Sulfide hand specimens were prepared for measurement by grinding and polishing a cut face down to a 6 μm diamond lap. The probe did not mark the pyrite surfaces, but left pits of diameter 20 to 70 μm and depth 1 to 30 μm in galena and chalcopyrite. In addition to the 'point' contacts on the polished surface, we used a large area contact fixed to the rough surface of the specimen by a silver impregnated silicone paste (Eccobond 59C from Emerson and Cuming Inc.)

Current for the measurement (0.1 to 10 mA) was supplied by batteries, and the voltage was measured with a Hewlett Packard 419A. A.C. pickup was reduced to about 4 μV by floating all circuitry and grounding the specimen through the large area contact.

The reported resistivity measurements (Table 1) were obtained by passing current through the outside two needle electrodes and measuring the voltage across the inner two electrodes (Wenner array). Linearity and reciprocity were routinely checked. To monitor sample homogeneity, adjacent electrodes were used for current and voltage (Dipole array), the probe was raised and lowered several times, and the sample was displaced several times transverse to the array, by a distance about equal to the array spacing. We considered the resistivity to be homogeneous when the results from all these measurements varied by less than a factor of 2. In many cases the variation was less than a fourth of the allowed range.

Thermoelectric voltage was measured between one of the needle electrodes and the large area base electrode. We used the convention that the thermopower (Seebeck coefficient) is positive when the gradients of voltage and temperature are in opposite directions, *i.e.,* when the hot electrode is electrically negative. The point electrode was heated by passing current through a fine wire wrapped around it. The values in Table 1 are for 40 mA current in 10 turns of #38 wire. From the magnitude of the voltage, the temperature difference was of the order of 1°C. The values given are strictly relative to the thermopower of steel (10 to 15 μV/°C), but this is small enough to be neglected. In a few cases only a sign is reported because the samples were used for other experiments before the quantitative thermoelectric measurements were made.

Spurious thermoelectric voltages on polished surfaces of galena, due to the polishing process, have been documented by Granville and Hogarth (1951). Tauc (1953) suggested that these were due to electrically charged mechanical damage in a surface layer. We found no evidence of such a surface layer effect, possibly because our probe load was an order of magnitude greater than theirs.

Resistivity distributions

The three sulfides being considered have a variable resistivity, due to variations in composition. To investigate the statistical distribution of resistivity in each case, we combined our data with all the previously published data we could find. In this way we reduced the statistical fluctuations due to limited sample number, and also averaged over many more localities. The histograms (Figs. 1, 2, and 3) include only resistivity measurements on natural specimens for which type was also determined and for which ancillary information indicated the measurements referred to a region of electrical and mineralogical homogeneity. Thus we excluded resistivity measurements on grains of mixed type and on polymineralic ores.

Figures 1 and 2 show that for both pyrite and galena *p*-type samples have a higher average resistivity than *n*-type samples, although the distributions overlap considerably. For pyrite (Fig. 2) the resistivity distributions seems to be log-normal, while for galena (Fig. 1) they are curiously flat, *i.e.,* have a negative kurtosis. The individual collections combined for Figures 1 and 2 do not differ significantly from the total resistivity distribution for given mineral and type. However, individual collections do differ significantly in the relative proportions of *n*-type and *p*-type. No homogeneous *p*-type galena samples were present in our collection, but in Figure 1 about one quarter of the galena samples are *p*-type.

For chalcopyrite all measurements meeting the given criteria were on *n*-type samples. However, *p*-type $CuFeS_2$ is known. Some of the synthetic specimens of Donovan and Reichenbaum (1958) were *p*-type, while Austin *et al.* (1956) and Olhoeft (personal communication, 1974) each report one natural *p*-type chalcopyrite. The individual collections used in Figure 3 do show significantly different resistivity distributions. More specifically, our values are distinctly higher than those reported by Parasnis (1956, p. 270). The respective modes are 3×10^{-3} ohm-m and 4×10^{-4} ohm-m. We attributed this to a difference in ore

TABLE 1. Sample descriptions and electrical data

Sample Site no.	Location	Deposit type*	Thermo-electric voltage (μV)	Resistivity ohm-meters*	Comments
	GALENA				
114,1	Edwards 3100 level D-7M Balmat, New York	Met.	-	Var.	Coarse to fine grained galena, minor pyrite, silicates.
117,1	5767 Bench, Berkeley Pit, Butte, Montana	HVP	Var.-	3.4×10^{-2}	Medium grained galena, minor pyrite, silicates; variable thermo-
117,2			Var.-	2.6×10^{-2}	electric voltage probably due to included phases.
118	Baxter Springs, Kansas	L.L.Z.	-403	9.6×10^{-5}	Coarse grained galena.
119,1	7100-7500 level, Hecla Star Mine, Wallace	HVR	-490	1.5×10^{-2}	Fine grained galena, silicates.
119,2	Coeur D'Alene	HVR	-480	5.5×10^{-3}	
119,3			-488	1.7×10^{-3}	
121	Lark Mine, Tintic, Utah	HVR	-620	1.7×10^{-2}	Coarse grained galena, minor chalcopyrite, quartz.
123,1	Lark Mine, Tintic, Utah	HVR	-	1.1×10^{-2}	Coarse grained galena.
123,2			-530	2.2×10^{-2}	
123,3			-	7.6×10^{-3}	
124,1	Butte, Montana	HVP	-290	6.2×10^{-5}	Coarse grained galena.
125,1	No. 29 Mine, St. Joe, Viburnum, Missouri	L.L.Z.	-	8.2×10^{-3}	Coarse grained galena, minor dolomite; variable thermo-
125,2			- +	9.7×10^{-3}	electric sign probably due to changes in chemistry; no indications of separate phases.
127,1	Broken Hill, Australia	Strat.	-300	1.2×10^{-4}	Coarse grained galena and sphalerite.
128,1	3850 level, Lucky Friday Mine, Coeur D'Alene	HV	-488	8.2×10^{-4}	Coarse to fine grained galena, minor chalcopyrite, silicates.
129,1	7700 level, Lucky Friday Mine, Coeur D'Alene	HV	-493	1.5×10^{-3}	Medium grained galena, minor tetrahedrite, quartz.
	PYRITE				
3,1	Bingham, Utah	HP	+185	5.0×10^{-1}	Single crystal, striations.
4,1	Dugway, Utah	HV	Var.-	5.3×10^{-2}	Single crystal, striations; variability in thermoelectricity due to separate phases.
5,1	Cactus Mine, Newhouse, Utah	HV	- +	Var.	Single crystal, striations, zone of concentric hemispherical holes.
6,1	Leadville, Colorado	HRV	+145	3.7×10^{-1}	Coarse grained pyrite, quartz crystals.
7,1	Sullivan, Missouri	Mag.H	-89	3.9×10^{-4}	Single twinned crystal, striated.
8,1	Sullivan, Missouri	Mag.H	-	1.9×10^{-5}	Coarse grained pyrite, magnetite,
8,2			-36	2.3×10^{-5}	minor chalcopyrite, silicates;
8,3			-	3.9×10^{-5}	thermoelectric voltage quite variable.
9,1	Sullivan, Missouri	Mag.H	-36	3.1×10^{-5}	Coarse grained pyrite.
10,1	6600' level South face,	HP	- +	3.1×10^{-1}	Medium to coarse grained vuggy
10,2	Bingham, Utah		- +	2.2×10^{-1}	pyrite, silicates; variable thermo-electric sign probably due to included phases.
11,1	6600' level South face,	HP	- +	7.3×10^{-1}	Medium to coarse grained vuggy
11,2	Bingham, Utah		- +	2.7	pyrite, silicates; variable thermo
11,3			- +	2.9×10^{-1}	electric sign probably due to included phases.
12,1	Geco, Ontario	Strat.	-98	4×10^{-2}	Medium grained granular pyrite,
12,2			- +	1.5×10^{-1}	silicates; variable thermoelectric sign probably due to included phases.
13,1	Geco, Ontario	Strat.	+	3.1×10^{-2}	Coarse grained pyrite, minor sphal-
13,2			minor -	4.7×10^{-2}	erite, chalcopyrite, galena, silicates; variable thermoelectric sign probably due to included phases.
14,2	4933 level, Berkeley Pit,	HVP	-	2.1×10^{-4}	Coarse grained pyrite, silicates;
14,3	Butte, Montana		-61	1.2×10^{-4}	chalcocite staining.
15,2	4933 level, Berkeley Pit,	HVP	-81	1.5×10^{-2}	Medium to coarse grained pyrite,
15,3	Butte, Montana		-84	2.1×10^{-3}	silicates; chalcocite staining.
16,1	4900 level, N. W. Series	HVP	-74	4.9×10^{-3}	Medium grained pyrite, silicates;
16,2	veins, Butte, Montana		-76	3.2×10^{-3}	chalcocite staining.
17,1	Leadville, Colorado	HRV	+153	3.5×10^{-2}	Single crystal, striations, fractured.
17,2			+	2.8×10^{-2}	
18,1	Phyllic Zone Diabase, Hayden, Arizona	HP	-83	3.1×10^{-3}	Medium grained pyrite, quartz.
19,2	2900 level, (Leonard Mine)	HVP	-65	1.8×10^{-3}	Fractured coarse grained pyrite,
19,3	Berkeley Pit, Butte, Montana		-	6.5×10^{-3}	quartz; chalcocite staining.
21,1	Balmat No. 2, 1900 sub level, Balmat, New York	Met.	-46	2.8×10^{-5}	Coarse grained pyrite, pyrrhotite, silicates.

Abbreviations as follows: H = hydrothermal; P = porphyry; R = replacement; V = vein, Var. = variable; Strat. = massive stratiform; L.L.Z. = limestone-lead-zinc; Mag. = magmatic; Met. = highly metamorphosed; Cont. = contact metamorphic.

TABLE 1, continued

Sample Site no.		Deposit type*	Thermo-electric voltage (μV)	Resistivity ohm-meters*	Comments
	CHALCOPYRITE				
301,1	Mt. Isa, Australia	Strat.	-363	2.2×10^{-4}	Fine grained chalcopyrite, silicates.
302,1	Park City, Utah	HVR	-465	5.1×10^{-3}	Coarse grained chalcopyrite, minor galena, silicates.
303,1	Timmins, Ontario	Strat.	-348	2.6×10^{-4}	Fine grained chalcopyrite
303,2			-350	3.4×10^{-4}	
304,1	Galena Mine, Wallace,	HVR	-	2.9×10^{-3}	Medium grained chalcopyrite, minor
304,2	Coeur D'Alene.		-	3.0×10^{-3}	pyrite and galena.
305,1	American Fork, Utah	HVR	-420	1.9×10^{-3}	Coarse grained chalcopyrite.
305,2			-408	1.7×10^{-3}	
306,1	Prescott, Arizona	Cont.	-334	9.9×10^{-4}	Coarse grained chalcopyrite, pyrite
306,2			-326	1.5×10^{-3}	quartz.
307,1	Jewel Stope, Jerome, Arizona	HR	-334	1.8×10^{-3}	Fine grained chalcopyrite with sub connected silicates.
308,1	Matahambre, Cuba	Strat.	-448	2.0×10^{-3}	Fine grained chalcopyrite.
309,1	Bingham, Utah	HP	-365	3.7×10^{-4}	Coarse grained chalcopyrite; chalcocite
309,2			-	3.6×10^{-4}	staining.
311,1	No. 29 mine, St. Joe,	L.L.Z.	-475	1.9×10^{-3}	Coarse to medium grained chalcopyrite,
311,2	Viburnum, Missouri		-	2.3×10^{-3}	vuggy quartz.
312,1	Geco, Ontario	Strat.	-347	2.3×10^{-4}	Medium grained chalcopyrite, pyrite.
312,2			-	1.6×10^{-4}	
313,1	Butte, Montana	HVP	-365	1.6×10^{-2}	Medium grained chalcopyrite, pyrite.
313,2			-435	1.6×10^{-2}	
314,1	Ore Zone Diabase, Hayden, Arizona	HP	-423	2.6×10^{-3}	Vein of medium grained chalcopyrite in diabase.
315,1	4500 level, Steward Mine,	HVP	-	2.6×10^{-1}	Medium grained chalcopyrite, minor
315,2	Butte, Montana		-	2.6×10^{-1}	pyrite.
315,3			-	3.0×10^{-1}	

environment. Our samples are mostly from the porphyry copper deposits of the western U.S., while those of Parasnis are from Swedish iron deposits. The same correlation was noticed by Harvey (1928, p. 799) who "observed that many low-resistance specimens came from mines that contained pyrrhotite, while many high-resistance specimens came from mines that contained bornite."

Mobility and carrier density

Resistivity is proportional to the product of carrier density and mobility (*e.g.*, Shuey, 1975, p. 46) so that the variations illustrated in Figures 1, 2, and 3 must be due to variations in mobility and carrier density. Where the deviations from stoichiometry and/or purity are known, carrier density can be calculated. Then, knowing the resistivity, the mobility can be calculated. The only samples of ours for which this is possible are pyrites #5 and #21 (Table 3). Here we can equate the density of carriers to that of Co atoms and then calculate mobility using the measured resistivity. For #21 the result is 5.5 $cm^2V^{-1}sec^{-1}$. Near site #8-2

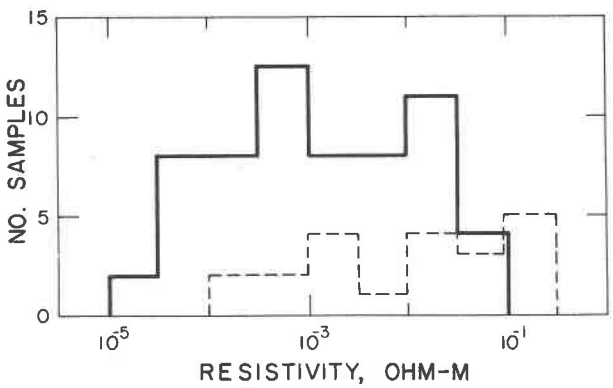

FIG. 1. Resistivity distribution for galena. Solid line is for *n*-type, dashed line is for *p*-type. Samples of mixed type are omitted. Based on the data in Table 1, the references to Figure 4, the 8 samples of Telkes (1950) and the 35 samples of Kireev *et al.* (1969).

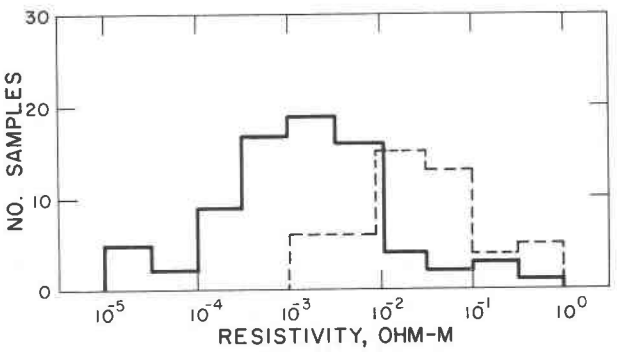

FIG. 2. Resistivity distribution for pyrite. Solid line is for *n*-type, dashed line is for *p*-type, and samples of mixed or uncertain type are omitted. Based on the data in Table 1 plus the following values: 22—Smith (1942); 2—Telkes (1950); 6—Marinace (1954); 20—Sasaki (1955); 20—Hill and Green (1962); 18—Kireev *et al.* (1969); 1—Fukui *et al.* (1971); 7—Ovchinnikov and Kirvoshein (1972); 6—Horita (1973).

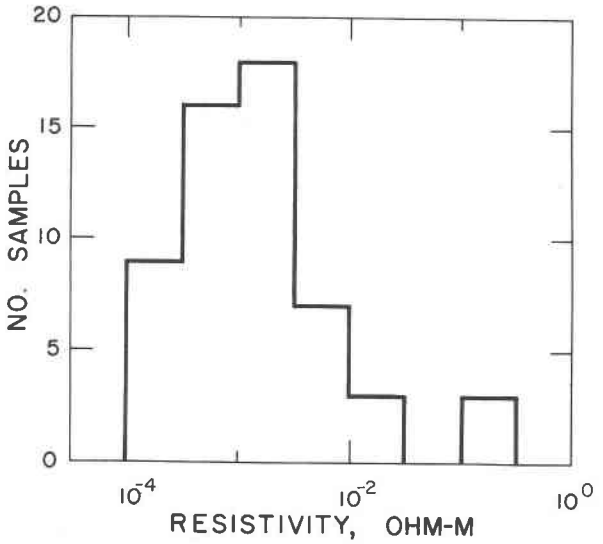

FIG. 3. Resistivity distribution for chalcopyrite. Besides the data in Table 1 this histogram includes published data as follows: 11—Telkes (1950); 3—Boltaks and Tarnovsky (1955); 7—Parasnis (1956); 4—Donovan and Reichenbaum (1958); 2—Frueh (1959); 1—Teranishi (1961); 4—Wintenberger (1968).

the Co averaged 0.3 wt percent and the computed mobility is 20 $cm^2V^{-1}sec^{-1}$.

For a given mineral, type, and temperature, there is a definite upper limit to the mobility, due to lattice vibrations. At room temperature these limits are approximately as follows, in units of $cm^2V^{-1}sec.^{-1}$: 600 for *n*-type and *p*-type galena, 150 for *n*-type pyrite, 20 for *n*-type chalcopyrite, and 2 for *p*-type pyrite. (See Shuey, 1975, for references). Mobility may be reduced by additional scattering due to point defects, dislocations, and grain boundaries. The range of mobility becomes smaller as the maximum theoretical value decreases. For *p*-type pyrite the lowest Hall mobility is about 0.5, one-fourth of the highest mobility.

There is no statistical difference between electron and hole mobilities in galena, so the difference in resistivity (Fig. 1) must be due to a difference in carrier density. This was recognized by Kireev *et al.* (1969) from their data on 33 samples. These together with 30 other samples of diverse origin are used in Figure 4. We find no statistically significant correlation of mobility with carrier density.

For pyrite there is no statistical difference in carrier density between *n*-type and *p*-type. This difference in resistivity (Fig. 2) is due entirely to the difference in mobility of electrons and holes.

Although there are relatively few published values of carrier density in chalcopyrite, the range is remarkably narrow, from 8×10^{18} cm^{-3} (Teranishi, 1961) to 4×10^{19} cm^{-3} (Donovan and Reichenbaum, 1958). This small range, together with the low value of the upper mobility limit, explains the relatively narrow distribution in Figure 3.

Correlation of resistivity and thermoelectricity

Under certain conditions the magnitude of the thermopower depends linearly on logarithm of carrier density, with a slope of -198 $\mu V/°C$ per decade (Tauc, 1962). One might expect therefore a high linear correlation of thermopower with logarithm of resistivity. Figures 5 and 6 show this is true for our data on galena and pyrite. *P*-type pyrite samples have systematically higher resistivity and higher thermopower than do *n*-type samples, since holes have a much larger effective mass and a smaller mobility than electrons. No correlation was observed for the data on chalcopyrite.

For a given mineral, type, and temperature, the thermopower depends on a second factor, the scattering mechanism. Thus in chalcopyrite where there is only a relatively small range in carrier concentration, the scattering mechanism becomes an important variable and the correlation between resistivity and thermopower disappears.

For pyrite and galena, a calibrated thermoprobe offers a rapid means of obtaining approximate resistivities on small volumes of sample.

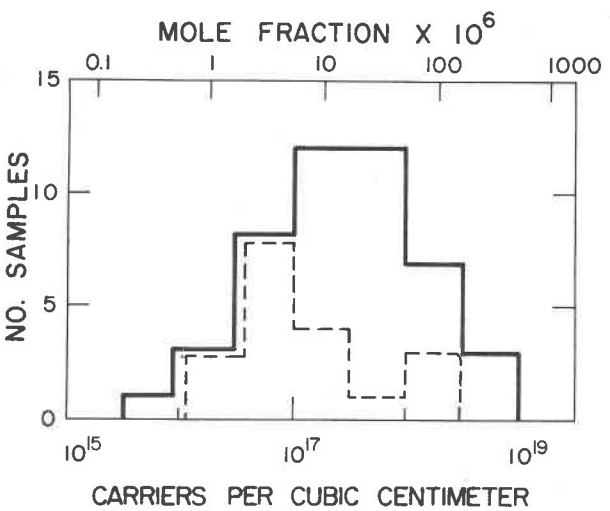

FIG. 4. Published carrier density in natural galena. Solid line is for *n*-type, dashed line is for *p*-type. The 63 values are from the following sources: 1—Brebrick and Scanlon (1954); 14—Putley (1955); 5—Finlayson and Grieg (1956); 2—Irie (1956); 5—Allgaier and Scanlon (1959); 2—Grieg (1960); 1—Farag *et al.* (1965); 33—Kireev *et al.* (1969).

Impurity

According to the principles of semiconductor physics, impurity atoms in solid solution generally have the following effects: a substitution of an element from the right in the periodic table constitutes a donor defect, and conversely a substitution of an element from the left constitutes an acceptor defect. Substitution from the same column, such as Se for S, has no effect other than slightly reducing the mobility. A metal interstitial is a donor, and anion interstitials are of negligible abundance. We did not consider impurities in chalcopyrite because of the evidence below that departure from stoichiometry has a greater influence on the carrier density.

Galena

For five galena samples chosen to span the full range of resistivity, the galena and included phases were scanned for Ag, Bi, Cu, and Sb (Table 2) with the microprobe (A.R.L. EMX-SM). In only one specimen, #129, were any of these elements detected in the galena. We did not notice any tendency for Ag and Sb concentrations to fluctuate synchronously. This is somewhat surprising in view of the extensive solubility of $AgSbS_2$ in PbS (Wernick, 1960). In the specimen with *p*-type regions (#125) no trace elements were detected in either *n*-type or *p*-type regions.

Pyrite

Nine pyrites of various types were analyzed for minor elements by a 3-meter Baird emission spectrograph (with a grating of 30,000 lines per inch) and by microprobe. The microprobe—sensitivity *ca.* 300–400 ppm for Co and Ni but much less for As—showed that only pyrites #8 and 21 contained Co, Ni, or As in solid solution. Samples of 40 mg for spectrographic analyses were secured by drilling, using a tungsten-carbide tipped bit, from the polished surfaces where the resistivity measurements had been made. These powders were ground and mixed with a germanium oxide buffer (one part sample, 3 parts buffer, total mass 16 mg) and fired with a D.C. arc of 12 amps. No tungsten was detected in any of the samples, so we assume there was no contamination from the bit. Semi-quantitative standards (1, 10, 100, 1000, 10000 ppm) were made by mixing spectrographically pure hematite and flowers of sulfur in the correct proportions for pyrite and pipetting in known amounts of impurities. Such a standard is not ideal because the sulfur is likely to come off earlier than for pyrite, thereby creating different matrix effects. The good agreement of spectrographic and probe results (for Co in samples #8 and #21) suggests the spectrograph standards were adequate for this study.

The spectrograph results (Table 3) for several samples showed Ag, Bi, and Cu to be present in amounts

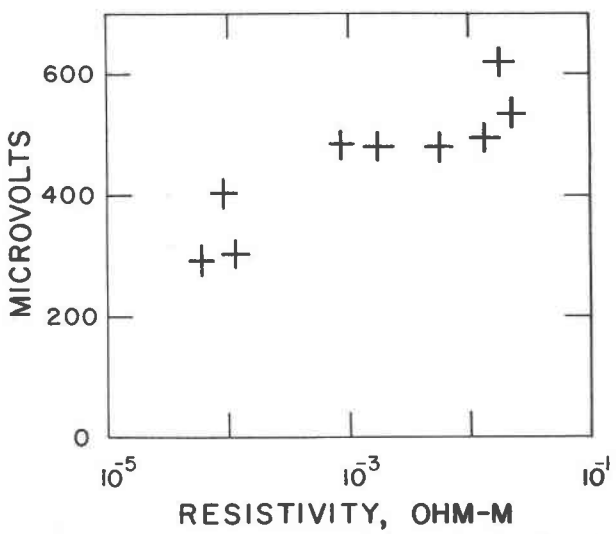

FIG. 5. Correlation of resistivity and thermoelectric voltage in galena. Data are from Table 1.

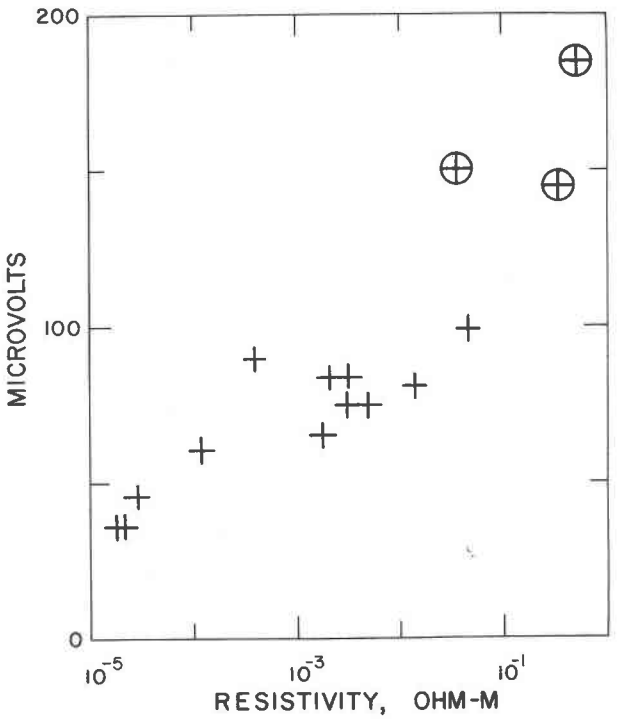

FIG. 6. Correlation of resistivity and thermoelectric voltage in pyrite. The circled marks are for *p*-type, the others are for *n*-type. Data are from Table 1.

TABLE 2. Microprobe results for Ag, Bi, Cu, Sb in galena

Sample	Carrier sign	Average resistivity ohm-meters	Comments
117	-	$3{\cdot}0x10^{-2}$	Chalcopyrite, pyrite, sphalerite grains. Exsolved phases of AgCu mineral (Jalpaite?) and Ag mineral (argentite?).
123	-	$1{\cdot}4x10^{-2}$	Sphalerite and pyrite grains.
124	-	$6{\cdot}2x10^{-5}$	No observable separate phases.
125	- +	$9{\cdot}0x10^{-3}$	No detectable change in Bi, Ag, Sb, Cu across areas where type changes. Exsolved Ag mineral (argentite?).
129	-	$1{\cdot}5x10^{-3}$	Exsolved SbCu(variable)Ag phases. Probably a member of tennantite - tetrahedrite series. Detectable Ag, Sb in lattice. Amount of Ag quite variable.

above the sensitivity limit of microprobe. Hence we returned to the probe and scanned for these elements. In no case were they detected in the pyrite. Instead they were found in small inclusions and (for Ag and Cu) filling cracks.

In Table 3 the four samples (#3, #5, #11, #17) lowest in Co are the four which are not definitely *n*-type. Three of them had no detectable Ni. This agrees with the statistics reported by Favorov *et al.* (1972). Also three of them have higher As than (Co + Ni), the exception being the one sample of these nine (#11) for which type could not be reliably determined.

The sample of mixed type (#5) was a single crystal with round holes about 30 to 70 μm in diameter, arranged in a zone about 1 mm wide and concentric with the edges of the crystal. The crystal is *n*-type in

TABLE 3. Pyrite impurity analyses

Pyrite No. Site	Resistivity ohm-meters**	Emission spectrograph analyses PPM Co	Ni	Ag	Cu	Mn	Bi	As	Sb	V	Ti	Microprobe results for Co, Ni, As, Bi, Ag, Cu and comments on polished section of sample.
n-type carrier sign -												
4,1	$5.3x10^{-2}$	100	90	>100	40	5	100	100	5	-	100	Minor unidentified p-type exsolved phase
8,1	$1.9x10^{-5}$	10,000	400	>>100	300	50	20	1000	5	-	1	Up to 10,000 ppm cobalt in structure, variable. Minor cracks contain cobalt. Small high silver phase in pyrite.
14,3	$1.2x10^{-4}$	100	5	>100	10,000	-	10	300	5	-	1	Intergranular bornite, covellite, chalcocite digenite.
18,1	$3.1x10^{-3}$	70	15	100	50	80	-	-	5	1	1	Intergranular silicates.
21,1	$2.8x10^{-5}$	1000	10	>100	30	40	-	200	-	1	1	1000 ppm cobalt in structure
p-type carrier sign +												
3,1	$5.0x10^{-1}$	50	-	>>>100	40	-	700	400	10	-	5	Exsolutions of CuAgBi mineral. Possibly a member of tennantite-tetrahedrite series.
17,2	$3.5x10^{-3}$	10	-	>100	500	-	40	100	-	-	1	No other observable phases. Copper present in major fractures.
mixed type carrier sign + -												
5,1	Var.	50	50	100	100	100	-	200	10	-	30	Hemispherical hole margins and some cracks high in silver. One hole margin high in copper.
questionable type												
11,1 11,2	{Average 1.7}	20	-	>>100	3000	-	3000	-	70	-	1	Chalcopyrite, chalcocite, bornite grains. Exsolved phase of BiCuAg mineral in pyrite.

* *Limits of detection (ppm) for spectrographic analyses were as follows: Co - 5; Ni - 1; Ag - <1; Cu - 1; Mn - 5; Bi - 10; As - 100; Sb - 1; V - 1; Ti - 1.*
** *Abbreviation: var. = variable.*

the vicinity of the cavities but *p*-type both at the surface and in the deep interior of the crystal (Fig. 7). Inward from the *p*-type zone the thermoelectric voltage is very erratic, indicating near equality of donor and acceptor concentrations. Radial zoning of this sort has been previously noted by Smith (1942, p. 7) and by Fischer and Hiller (1956, p. 287). The microprobe showed Ag (and in one case Cu) on the edges of the cavities, and also in some cracks. No impurities were detected in the pyrite, either in *n*-type or *p*-type regions. One possible interpretation of our data for pyrite #5 is as follows: The crystal initially grew as *p*-type, due to content of As (and possibly Mn). Then the content of Ag and Cu increased, these acting as donors to compensate the As acceptors. Then a Ag-rich phase precipitated in the growing pyrite, which by this time was completely *n*-type. For a final stage of growth the initial conditions were repeated. The Ag-rich phase was later eroded out leaving the cavities, and possibly at this time Ag was deposited in some cracks.

Among the five *n*-type pyrites of Table 3, the two outstandingly low in resistivity (#8, #21) are also the two rich enough in cobalt for the probe to prove its presence in the pyrite structure. For sample #21 the Co content was fairly uniform at 1000 ppm = 0.1 wt percent = 0.2 at percent. By contrast, in pyrite #8

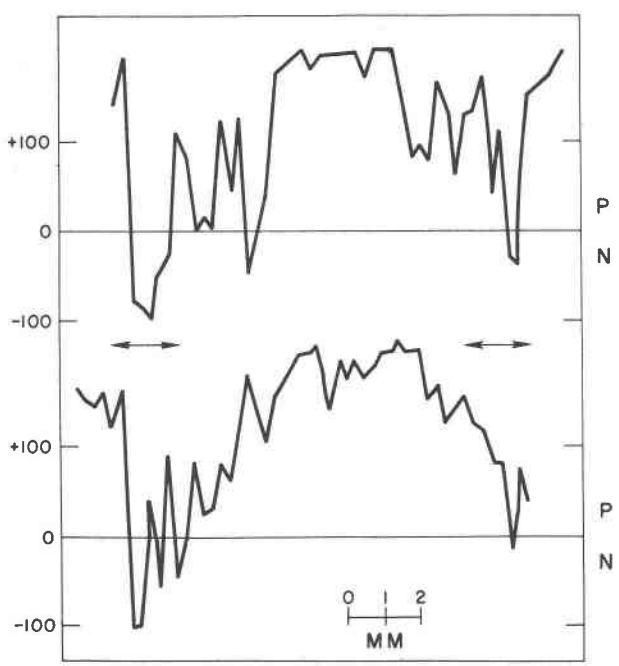

FIG. 7. Two typical profiles of thermoelectric voltage (in microvolts) across pyrite sample #5. Arrows show the zone of round cavities.

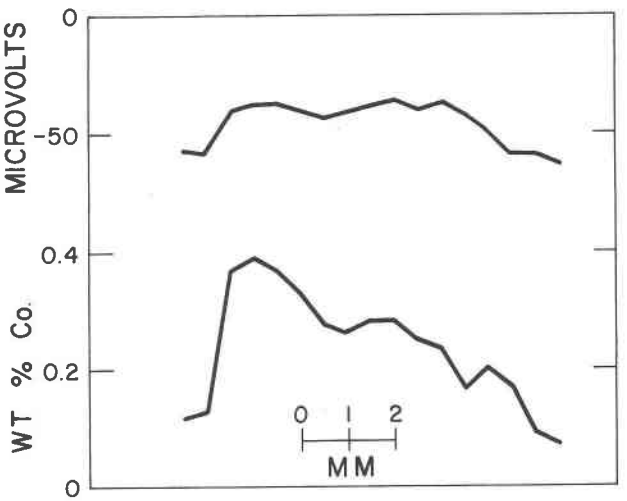

FIG. 8. Thermoelectric voltage (above) and wt percent cobalt (below) along the same profile in pyrite #8. The microprobe results for Co are the average of two traverses.

cobalt concentration varied from over 1 to 0.06 wt percent. Figure 8 shows how the thermoelectric voltage varies synchronously with Co content. This data is in accord with theory (Tauc, 1962) if we assume a temperature difference of 1°C and an effective electron mass of 0.1 times the free-electron mass. This latter value is also implied by the thermoelectric and the Hall effect data of Bither *et al.* (1968) on one sample of synthetic *n*-type FeS_2.

Comparison of data for pyrites #4 and #14 illustrates the importance of Cu as a donor. Pyrite # has Co + Ni > As without any of the impurity concentrations being very high. It is accordingly *n*-type with fairly high resistivity. In pyrite #14 the spec analyses show (Co = Ni) < As which would suggest *p*-type semiconduction. But this sample is evidently saturated with Cu, based on the extraordinary high Cu analysis and the presence of various Cu-rich minerals. The observed large *n*-type conductivity must be attributed to the donor effect of Cu.

Discussion

The lower limit of detection with spectrographic analysis is about 10^{16} cm^{-3} for most impurities, though somewhat higher for As (about 10^{18} cm^{-3}). In galena and pyrite this is near the lower limit of carrier density (*cf* Fig. 4). Although the spectroscope has sufficient sensitivity for most impurities, many sulfide specimens contain microscopic to submicroscopic inclusions which will contaminate any microsampling of the specimen. Sampling with the microprobe is

much more reliable, but the lower limits of detection are close to 10^{19} cm^{-3}. In galena or pyrite, carrier densities this large are exceptional (*cf* Fig. 4).

The measurements reported above suggest that, with few exceptions, large spectrographic impurity levels indicate contamination by separate phases. The correlations reported by other authors between type and impurities (Hiller and Smoczyk, 1953; Fischer and Hiller, 1956, Favorov *et al.*, 1972) may strictly represent correlations with microscopic to submicroscopic inclusions containing these impurities. Of course trace elements present in separate phases are likely present in solid solution in the host as well. Within these limitations, our results for pyrites from North American deposits agree with previously published results from deposits in Germany (Fischer and Hiller, 1956) and Russia (Favorov *et al.*, 1972). Specifically the important donor impurities are Ni, Co, and Cu, while As is the most important acceptor impurity. Low resistivity occurs in pyrite if a single impurity is present in significantly greater concentration than other impurities. Roughly equal concentrations of donor and acceptor defects gives a high resistivity (*e.g.*, pyrite #4).

Nonstoichiometry

A metal excess (sulfur deficiency) corresponds to a donor defect (*n*-type semiconduction) and a metal deficiency (sulfur excess) corresponds to an acceptor defect (*p*-type semiconduction). This is true regardless of whether the atomic mechanism in either case is a vacancy or an interstitial. These defects are always present to some extent, because only a finite energy is needed to create them. Thus in practice a mineral is never stoichiometric. The maximum deviation in a homogeneous phase will depend somewhat on temperature of atomic equilibration. It may however be too small to resolve by chemical analysis, while at the same time large enough to account for the observed electrical charge carriers. This is the situation in all three of the minerals under consideration.

Galena

The electrical effects of deviations from stoichiometry in galena have been well studied by Bloem and Kroeger (1956). Their results show that the composition can deviate in either direction depending on temperature and sulfur pressure. Lowering the temperature at fixed sulfur pressure changes the equilibrium composition from *n*-type to *p*-type.

Pyrite

It seems that at high temperature and a broad range of sulfur pressures, pure pyrite is *n*-type. Crystals produced near 700°C by Bittner (1950) from a bromide melt and by Bither *et al.* (1968) using chlorine transport were all *n*-type. We heated a portion of our sample #17 for a week at 500°C in a closed vessel (free volume about 100 times sample volume). This sample was initially *p*-type, and our purpose was to create donors by driving off sulfur. After heating, the sample was not quenched but rather allowed to cool naturally. There was no type change but resistivity did increase, suggesting that donors had been created to compensate the acceptors initially present. Resistivity measurements ranged from 4.7 to 4.9 $\times$ 10^{-2} ohm-m before heating, and from 6.5 to 7.4 $\times$ 10^{-2} after heating. When we repeated the experiment at 550°C, the sample shattered with visible sulfur loss. We could not then measure resistivity, but the type had not changed. Bittner (1950, p. 184) reported that in some cases he was able to change *p*-type to *n*-type by driving off sulfur, but he gives no details.

It is not clear whether there is a *p*-type portion of the pyrite field at high temperature. We could not produce a change in type by annealing an *n*-type sample at 550°C with excess sulfur. However, Bittner (1950, p. 183) reported he could change natural *n*-type pyrite to *p*-type by heating in a closed evacuated vessel near 700°C and removing the pyrrhotite formed.

Chalcopyrite

Metal in excess of stoichiometric $CuFeS_2$ is indicated as a donor defect because of persistent reports of an irreversible decrease in resistivity upon heating (references in Shuey, 1975, p. 248). It is plausible to suppose that the characteristic *n*-type conduction is a consequence of the characteristic slight metal excess (Barton, 1973). The natural range of carrier density (see below) corresponds to a metal excess on the order of 0.1 percent. The ratio of iron to copper in chalcopyrite may also deviate from stoichiometric $CuFeS_2$. Comparison between our resistivity measurements and those previously published suggests that iron substituted for copper will have a donor effect, while substituting copper for iron will create acceptors. This hypothesis is not at all inconsistent with the established donor effect of Cu substituted for Fe in pyrite, because of the differences in band structure (Shuey, 1975, p. 249, 313).

In an attempt to verify this prediction, we coated chalcopyrite sample #304-2 with copper paint and heated it in an evacuated vessel at 150°C for 4 months. This low temperature was chosen because of the published report of irreversible sulfur loss at 200°C (Donovan and Reichenbaum, 1958). Light repolishing after heating removed less than 1 mm of material. The measured resistivity was the same as previously measured (Table 1). No definite inference can be made, but a likely explanation is that the diffusion of copper was too slow for penetration to the depth probed in the resistivity measurement.

Geochemistry of charge carriers

The main motivation for the measurements and statistical analyses reported in this paper was to understand the geologic factors controlling the density of free charge carriers. We are led to certain conclusions, which should be regarded as working hypotheses, to be tested and revised by future work.

Galena

Our suite contained no *p*-type galena and only one mixed-type galena (#125). Therefore, we analyzed the localities given in the literature for *p*-type galena. Besides the references to Figures 1 and 4 we consulted Hiller and Smolczyk (1953) and Smolczyk (1954), who determined type (but not resistivity) on 57 galena samples of diverse origin. We found without any definite exception that *p*-type galena is restricted to two kinds of deposits, namely stratabound limestone-lead-zinc ("Mississippi Valley") deposits and also those deposits considered notably argentiferous. In both cases *n*-type and mixed-type occur with the *p*-type, all with comparable abundance. The acceptor defects in galena are Pb vacancies and Ag substituting for Pb. In the argentiferous deposits it is natural to assume that Ag in solid solution is the dominant acceptor. The stratabound limestone-lead-zinc deposits are "characteristically very low in silver" (Stanton, 1972, p. 548). By elimination, Pb vacancies are indicated. This also makes sense because limestone-lead-zinc deposits were formed at low temperature, and the extensive experiments of Bloem (1956) showed that lowering temperature (at constant sulfur fugacity) results in lead-deficient equilibrium galena composition. But the observation of exsolved silver sulfide in galena #125 (Table 2) is a reminder of caution.

Pyrite

Because pyrite occurs in almost any type of geologic environment, no simple analysis can be adequate for the factors influencing type and density of carriers. We are aware of more than a dozen publications on this subject, but the question is far from resolved. It seems to us that in many situations the relevant defects are the donor impurities Co, Ni, Cu, and the acceptor impurity As. The studies on our limited suite certainly support this. It can no longer be supposed, as Smith (1947) in effect presumed, that carrier type and density are unique functions of formation temperature. Yet it seems that two patterns originally recognized by Smith have been substantiated by subsequent investigations. First, pyrite from sedimentary and epithermal deposits is *p*-type with remarkable consistency, provided cupriferous sediments are excluded. For example, Favorov *et al.* (1972, Table 2) show all *p*-type for a lead-zinc deposit at Blagadatskoie (1616 samples) and also for a deposit at Tsentral'noie with colloform pyrite (2073 samples). At Gilman, Colorado, Lovering (1958) identified pyrite deposited before and after the main mineralization. The later pyrite, with interpreted formation temperature below 150°C, was all *p*-type. What is not established is whether the dominant acceptor is iron deficiency or arsenic impurity. (It should be remembered that arsenic can contribute almost 10^{18} cm^{-3} carriers yet be undetectable in spectrographic analyses).

The second pattern, first shown by Smith's data, is that pyrite from high-temperature veins is *n*-type with remarkable consistency, provided arsenopyrite is not in the assemblage. As an example, Hill and Green (1962) found only *n*-type (38 samples) in the mineralized quartz-porphyry dikes of Mt. Bischoff, Tasmania, where the pyrite was formed with cassiterite. Karasev *et al.* (1972, Table 2) show only *n*-type (784 samples) from a tungsten deposit at Kholtosonskoe. They imply the probable cause is sulfur deficiency due to high formation temperature.

Chalcopyrite

The evidence available to date gives no indication that impurities have any important effect on the resistivity and type of chalcopyrite. Natural *p*-type samples are rare, apparently because of the donor effect of excess metal. Copper substituting for iron may produce acceptors which compensate some of the donors, decreasing the carrier concentration and

so increasing the resistivity. However, this has not yet been demonstrated by direct experimentation.

Acknowledgments

This research was supported by NSF Grant GA 31571 to S. H. Ward. One of us (D.F.P.) was also assisted by graduate fellowships from the American Smelting and Refining Company and from the Commonwealth Scientific and Industrial Research Organization (Australia).

For assistance in collection of specimens we thank R. Miller and D. Gustafson (Anaconda Company, Butte, Montana), J. Emery (Meremec Mining Company, Sullivan, Missouri), D. B. Dill, Jr. (St. Joe Minerals Corporation, Balmat, New York), H. E. Myers and R. G. Dunn, Jr. (St. Joe Minerals Corporation, Bonne Terre, Missouri), S. H. Huff (ASARCO, Wallace, Idaho), J. Simos (Hecla Mining Company, Wallace, Idaho), J. D. Stevens and S. A. Hoelscher (Kennecott Copper Corporation, Salt Lake City, Utah, and Ray Mines Division, Hayden, Arizona), R. Pemberton and R. Weeks (Noranda Mines Limited, Ontario, Canada).

The help of J. Haselton in making the microprobe measurements and F. Jensen in sample preparation is gratefully acknowledged. We are indebted to Kennecott Exploration Inc. for the use of their spectroscope facilities, and particularly to S. Cone for help in making these measurements.

References

Allgaier, R. S., and W. W. Scanlon (1958) Mobility of electrons and holes in PbS, PbSe, and PbTe between room temperature and 4.2°K. *Phys. Rev.* **111,** 1029–1037.

Austin, I. G., C. H. L. Goodman, and A. E. Pengally (1956) New semiconductors with the chalcopyrite structure. *J. Electrochem. Soc.* **103,** 609–610.

Barton, P. B. (1973) Solid solutions in the system Cu–Fe–S. Part II: The Cu–S and Cu–Fe–S joins. *Econ. Geol.* **68,** 455–465.

Bither, T. A., R. J. Bouchard, W. H. Cloud, P. C. Donohoe, and W. J. Siemons (1968) Transition metal dichalcogenides. High-pressure synthesis and correlation of properties. *Inorg. Chem.* **7,** 2208–2220.

Bittner, J. (1950) On the rectification characteristics of synthetic pyrite. *Jenaer Zeiss-Jahrb.* **1950,** 177–185 (in German).

Bloem, J. (1956) Controlled conductivity in lead sulfide single crystals. *Phillips Res. Rep.* **11,** 273–336.

———, and F. A. Kroger (1956) The *P-T-X* phase diagram of the lead-sulfur system. *Z. Phys. Chem.* **7,** 1–14.

Boltaks, B. I., and N. N. Tarnovsky (1955) Electrical properties of chalcopyrite. *Zh. Teckh. Fiz.* **25,** 402-409 (in Russian).

Brebrick, R. F., and W. W. Scanlon (1954) Electrical properties and the solid-vapor equilibrium of lead sulfide. *Phys. Rev.* **96,** 598–602.

Donovan, B., and G. Reichenbaum (1958) Electrical properties of chalcopyrite. *Brit. J. Appl. Phys.* **9,** 474–477.

Farag, B. S., I. A. Smirnov, and Y. L. Yousef (1965) Thermal and electrical properties of natural monocrystals of lead sulfide. *Physica,* **31,** 1673–1680.

Favorov, V. A., V. I. Krasnikov, and V. S. Sychugov (1972) Some factors defining the variability of semiconducting qualities of pyrite and arsenopyrite. *Izvest. Akad. Nauk SSSR, Ser. Geol.* **11,** 72–84 (in Russian).

Finlayson, D. M., and D. Grieg (1956) Electrical measurements on natural galena at low temperature. *Proc. Phys. Soc.* **69B,** 796–801.

Fischer, M., and J. E. Hiller (1956) On the thermoelectric effect of pyrite. *Neues Jahrb. Mineral.* **89,** 281–301 (in German).

Frueh, A. J. (1959) Use of zone theory in problems of sulfide mineralogy, part II; the resistivity of chalcopyrite. *Am. Mineral.* **44,** 1010–1019.

Fukui, T., T. Miyadai, and S. Miyahara (1971) Photoconductivity of natural pyrite. *J. Phys. Soc. Japan,* **31,** 1277.

Granville, J. W., and C. A. Hogarth (1951) A study of thermoelectric effects at the surfaces of transistor materials. *Proc. Phys. Soc.* **64B,** 488–494.

Grieg, D. (1960) Thermoelectricity and thermal conductivity in the lead sulfide group of semiconductors. *Phys. Rev.* **120,** 358–365.

Harvey, R. D. (1928). Electrical conductivity and polished mineral surfaces. *Econ. Geol.* **23,** 778–803.

Hill, P. A., and R. Green (1962) Thermoelectricity and resistivity of pyrite from Renison Bell and Mt. Bischoff, Tasmania. *Econ. Geol.* **57,** 579–586.

Hiller, J. E., and H. G. Smolcyzk (1953) Spectroanalytic investigations on galena with consideration of photoelectric, thermoelectric, and rectification effects. *Z. Elektrochem.* **57,** 50–58 (in German).

Horita, H. (1973) Some semiconducting properties of natural pyrite Japan. *J. Appl. Phys.* **12,** 617–618.

Irie, T. (1956) Magnetoresistance effect of lead sulfide semiconductors I. Measurements on natural specimens of lead sulfide. *J. Phys. Soc. Japan,* **11,** 840–846.

Karasev, A. P., V. I. Krasnikov, V. D. Pantaev, R. S. Seifullin, V. S. Sychugov, and V. A. Favorov (1972) Some electriophysical properties of East Trans-Baikalian pyrite. *Akad. Nauk. SSSR, Sibirskoe Otdelenie, Geol. Geofiz.* **5,** 64–71 (in Russian).

Kireev, P. S., A. P. Korovin, V. I. Krasnikow, N. A. Muravey-nik, V. D. Pantaev, V. S. Sychugov, R. S. Seifullin, and V. A. Favorov (1969) The Hall effect of some East Baikal ore mineral deposits. *Izv. Akad. Nauk SSSR, Ser. Geol.* **6,** 75–82 (in Russian).

Lovering, T. G. (1958) Temperatures and depth of formation of sulfide ore deposits at Gilman, Colorado. *Econ. Geol.* **53,** 689–707.

Marinace, J. C. (1954) Some electrical properties of natural crystals of iron pyrite. *Phys. Rev.* **96,** 593.

Ovchinnikov, I. K., and A. A. Krivoshein (1972) Temperature dependence of the Hall coefficient and electrical conductivity of pyrites in the temperature range of −150°C to 500°C. *Izvest. Akad. Nauk. SSSR, Fiz. Zemli,* **11,** 86–90. (Translation: *Izvestia, Phys. Solid Earth,* 766–769).

Parasnis, D. S. (1956) The electrical properties of some sulfide and oxide minerals and their ores. *Geophys. Prospect.* **4,** 249–278.

Putley, E. H. (1955) The Hall coefficient, electrical conductivity, and magnetoresistance effect of lead sulfide, selenide, and telluride. *Proc. Phys. Soc.* **68B,** 22–34.

Sasaki, A. (1955) On the electrical conduction of pyrite. *Mineral. J.* **1,** 290–302.

Shuey, R. T. (1975) *Semiconducting Ore Minerals.* Elsevier Publishing Co., Amsterdam.

Smith, F. G. (1942) Variation in the properties of pyrite. *Am. Mineral.* **27,** 1–19.

SMITH, F. G. (1947) The pyrite geothermometer. *Econ. Geol.* **42,** 515–523.

SMOLCZYK, H. G. (1954) The influence of sulfur concentration and of antimony content on lead sulfide photoelements. *Z. Elektrochem.* **58,** 263–270 (in German).

STANTON, R. L. (1972) *Ore Petrology.* McGraw Hill, New York.

TAUC, J. (1953) An explanation of some anomalous thermoelectric phenomena on the surface of transistor materials. *Czech. J. Phys.* **3,** 259.

——— (1962) *Photo and Thermoelectric Effects in Semiconductors.* Pergamon Press, New York and Oxford.

TELKES, M. (1950) Thermoelectric power and electrical resistivity of minerals. *Am. Mineral.* **35,** 536–555.

TERANISHI, T. (1961) Magnetic and electric properties of chalcopyrite. *J. Phys. Soc. Japan,* **16,** 1881–1887.

WERNICK, J. H. (1960) Constitution of the $AgSbS_2$–PbS, $AgBiS_2$–PbS, and $AgBiS_2$–$AgBiSe_2$ systems. *Am. Mineral.* **45,** 591–598.

WINTENBERGER, M. (1957) Measurement of electrical conductivity of crystals, case of chalcopyrite. *C. R.* **244,** 1801–1803 (in French).

Manuscript received, September 16, 1974; accepted for publication, September 26, 1975.